JAAS

ROYAL SOCIETY OF CHEMISTRY

PAPER

View Article Online
View Journal | View Issue

Cite this: *J. Anal. At. Spectrom.*, 2023, **38**, 1192

A new double spike method for the determination of mass-dependent Te isotope compositions of meteorites and terrestrial materials by MC-ICP-MS

Elin M. Morton, *[a] Katharina Kreissig,[a] Barry J. Coles,[a] Caris S. Jaffe,[a] Rayssa Martins,[a] Graeme M. Poole[ab] and Mark Rehkämper[a]

This study presents a new method for the determination of mass-dependent Te isotope compositions. The process encompasses a new column chromatographic procedure which separates Te from chondritic and iron meteorites and diverse terrestrial rocks with high yield and purity, combined with a robust ^{125}Te–^{128}Te double spike and optimised multi collector ICP-MS protocols. This allows for precise (2SD = 0.07‰) determination of the mass-dependent ^{130}Te/^{125}Te isotope ratio using analyte solutions containing as little as 6 ng of natural Te. The efficacy of the method is demonstrated by repeat analyses of terrestrial rock reference materials and meteorites, which show overall good agreement with previous work. In addition, an inter-laboratory cross-calibration of three different Te standard solutions was performed. This inter-laboratory cross-calibration is highly advantageous, as a well-calibrated isotope reference material is not yet available for Te. Isotope mass balance and mixing equations performed in this study show that hypothetical mass-independent Te isotope effects of reasonable magnitude are unlikely to have a significant impact on the measured mass-dependent Te isotope compositions at the current level of analytical precision. Finally, this study presents the first precise mass-dependent Te isotope composition obtained for an iron meteorite, Canyon Diablo, and komatiite reference material KAL-1 using the double spike technique.

Received 16th March 2023
Accepted 18th April 2023

DOI: 10.1039/d3ja00091e

rsc.li/jaas

Introduction

Tellurium is a chalcophile and moderately volatile trace element with a 50% condensation temperature of 655 K, which has 8 stable isotopes with atomic mass numbers between 120 and 130.[1] Previous investigations have shown that Te is vulnerable to stable isotope fractionation during nebular and parent body processes, such as partial evaporation/condensation, thermal metamorphism, and aqueous alteration, and Te isotopes can, therefore, be used to investigate such processes through analyses of meteorites.[2–4] The mass-dependent Te isotope compositions of terrestrial samples have also received attention in recent years as they may be of use as a proxy for ancient marine and terrestrial redox conditions. Additionally, as a chalcophile element, Te is of interest for investigating the genesis of metal-bearing ore systems, and as an ore exploration tool. Mass-dependent Te isotope fractionation is especially interesting in exploration for high-grade Au mineralisation due to the close association of Te with Au in ore bodies.[2,3,5–9]

Fornadel *et al.* (2014)[5] developed methods for analyses of the mass-dependent Te isotope compositions of ores and ore-related minerals by multi collector ICP-MS (MC-ICP-MS) by expanding on the methodologies presented in Fehr *et al.* (2004).[10] In contrast to stable isotope studies of other elements, Fornadel *et al.* (2014)[5] did not use a double spike, but instead utilised Cd as an external dopant to correct for instrumental mass bias.

The first studies that employed the double spike technique to investigate the mass-dependent Te isotope compositions of meteorites and terrestrial samples were by Fehr *et al.* (2018)[2] and Fukami *et al.* (2018).[8]

Fukami *et al.* (2018)[8] determined Te and Se concentrations and mass-dependent Te isotope composition of several reference materials using a ^{125}Te–^{128}Te double spike and MC-ICP-MS. They found that Te/Se ratios covaried with the mass-dependent Te isotope data and hence suggested that Te may be useful as a redox proxy. This was expanded on by Wasserman and Johnson (2020)[9] who investigated mass-dependent Te isotope compositions for a range of terrestrial samples using hydride generation MC-ICP-MS and a ^{120}Te–^{124}Te double spike. They found significant mass-dependent Te isotope fractionations in low-temperature terrestrial and marine environments, which they tentatively attributed to redox reactions or adsorption.[8,9]

Fehr *et al.* (2018)[2] developed new ^{125}Te–^{128}Te double spike and MC-ICP-MS protocols to investigate the mass-dependent Te isotope compositions of meteorites and terrestrial samples and found significant isotopic fractionation for both. Notably, this included substantial within-group variations in the mass-

[a]*Department of Earth Science and Engineering, Imperial College London, London SW7 2AZ, UK. E-mail: e.rydeblad18@imperial.ac.uk*
[b]*Imaging and Analysis Centre, Natural History Museum, London SW7 5BD, UK*

dependent Te isotope compositions of carbonaceous chondrites.

Hellmann *et al.* (2020)[3] used similar Te purification and MC-ICP-MS protocols as Fehr *et al.* (2018)[2] but employed a ^{123}Te–^{125}Te double spike. In contrast to Fehr *et al.* (2018),[2] Hellmann *et al.* (2020)[3] found little to no within-group variations in the Te isotope compositions of carbonaceous chondrites. Instead, they identified coupled between-group differences of mass-dependent Te isotope compositions and concentrations, which they ascribed to variable mixing between a matrix rich component and chondrules or chondrule pre-cursors.[3]

Despite these recent studies that investigate mass-dependent Te isotope compositions, numerous important questions remain unresolved. In particular, only limited results are currently available to constrain the mass-dependent Te isotope composition of the bulk silicate Earth (BSE), whilst the Te isotope compositions of several chondritic meteorite groups have not been fully investigated, and data is completely lacking for achondrites and iron meteorites.[2,4] As such, further analyses of both terrestrial samples and meteorites are needed to better constrain the chondrite group(s) that contributed to Earth's late veneer.[2,3] Additionally, resolving the impact of different oxidation states on the behaviour of Te during isotope fractionation would enable the application of Te isotopes as an effective tracer of redox and volatile element fractionation processes in terrestrial and extra-terrestrial environments.[2,5–9]

This study presents improved procedures for the determination of mass-dependent Te isotope compositions by MC-ICP-MS. The procedures employ a ^{125}Te–^{128}Te double spike, which was developed for this study, coupled with optimised chromatographic procedures that enable separation of Te from silicate rocks as well as stony and iron meteorites with near-quantitative yields and a near-complete separation from elements that generate spectral interferences, including Sn and Cd. The methods are validated by analyses of synthetic samples with known isotope compositions as well meteorites and terrestrial samples that were previously analysed in other laboratories and an intercalibration between the different Te isotope reference materials that were employed. In addition, we also report the first mass-dependent Te isotope compositions obtained using the double spike technique for an iron meteorite, Canyon Diablo, and the komatiite reference material KAL-1.

Methods

Reagents and materials

All sample preparation work was carried out in the ISO Class 6 clean rooms of the MAGIC Laboratories at Imperial College London, with blank-sensitive steps performed in ISO Class 4 laminar flow hoods. All mineral acids (HCl, HNO_3, and HF) were purified in-house by sub-boiling distillation and all water used was of ≥18.2 MΩ cm grade sourced from a Millipore purification system. Samples and Te standard solutions were stored either in Teflon bottles or Savillex PFA vials before, during, and after processing. The Savillex PFA vials were cleaned by three subsequent complete submersion steps, first in 8 M HNO_3, followed by 6 M HCl, and finally in a mixture of ≥18.2 MΩ cm grade H_2O, distilled 6 M HCl, and distilled 15 M HNO_3. During each submersion step, the vials were allowed to soak in the acid or acid-water mixture for 72 to 96 hours at approximately 100 °C.

Te standard solutions and data notation

A London Te solution that was prepared in-house was used as the primary Te isotope reference material in this study. Briefly, the London Te standard solution was prepared by dissolving 32.8 mg of 99.9999% pure Te (Alfa Aesar, lot number T11E031). The Te standard solution was then made up to a Te concentration of about 33 μg g^{-1} by dilution, using 6.5 M HCl.

To facilitate inter-laboratory comparison, three further Te isotope reference materials from two other laboratories were also analysed. In detail, M. Fehr from ETH Zürich provided aliquots of a NIST SRM 3156 Te standard solution (Lot. no. 892901; termed NIST-ETH Te in the following) and a Te standard solution prepared from Alfa Aesar elemental Te (termed AA-ETH Te in the following). In addition, J. Hellmann from the University of Münster provided an aliquot of their NIST SRM 3156 Te standard solution (Lot. no. 140830; named NIST-Münster Te in the following).

This study uses the δ-notation to report the mass-dependent Te isotope compositions of the measured samples. In detail, the notation denotes the relative deviation of the ^{130}Te/^{125}Te isotope ratio determined for a sample from the value measured for a standard reference material (standard) in parts per 1000 (‰):

$$\delta^{130}\mathrm{Te} = \left(\left[\frac{\left(^{130}\mathrm{Te}/^{125}\mathrm{Te}\right)_{\mathrm{sample}}}{\left(^{130}\mathrm{Te}/^{125}\mathrm{Te}\right)_{\mathrm{standard}}} \right] - 1 \right) \times 10^3 \quad (1)$$

To facilitate direct comparisons between the results of this study and previously published literature that use a $\delta^{128/126}$ notation, the following equation was used for the conversion of delta values:

$$\delta\mathrm{Te_A} = ([\delta\mathrm{Te_B}/1000 + 1]^{\beta} - 1) \times 10^3 \quad (2)$$

Where $\delta\mathrm{Te_A}$ is the δTe value for the isotope ratio ^{A1}Te/^{A2}Te, and $\delta\mathrm{Te_B}$ is the δTe value for the isotope ratio ^{B1}Te/^{B2}Te. The β term is calculated using eqn (3):

$$\beta = \frac{\ln(m_{\mathrm{A1}}/m_{\mathrm{A2}})}{\ln(m_{\mathrm{B1}}/m_{\mathrm{B2}})} \quad (3)$$

Here m_{A1}, m_{A2} denote the atomic masses of the isotopes in $\delta\mathrm{Te_A}$ and m_{B1}, m_{B2} denote the masses of the isotopes in $\delta\mathrm{Te_B}$.[11] Conversion of δ^{130}Te values that are referenced to different Te standard solutions was carried out using the simplified approach of Rehkämper *et al.* (2011),[12] shown below using AA-ETH as an example:

$$\delta^{130}\mathrm{Te_{London}} \approx \delta^{130}\mathrm{Te_{(AA\text{-}ETH)}} + \Delta^{130}\mathrm{Te_{(AA\text{-}ETH)\text{-}London}} \quad (4)$$

Te double spike

Double spike design and preparation. With eight stable isotopes Te is well suited for measurements of mass-dependent

isotope fractionations by way of the robust double spike technique. Briefly, the double spike technique stipulates that the true mass-dependent isotope composition of a sample can be mathematically calculated by measuring four separate isotopes, where the abundances of two isotopes are artificially enhanced in the sample by the addition of a double spike of known composition.[13]

The choice of isotopes that were used for the double spike and data reduction in this study was guided by the error propagation models of Rudge *et al.* (2009)[13] and made with the aim to (i) minimise the error on the natural mass-fractionation factor (α) and (ii) avoid large isobaric interference corrections.[13] Hence, in accord with previous studies, a ^{125}Te–^{128}Te double spike was prepared for, and employed in, this study.[2,8] This allows the four most abundant Te isotopes – ^{125}Te, ^{126}Te, ^{128}Te, and ^{130}Te – to be used in the double spike inversion in the form of ^{126}Te/^{125}Te, ^{128}Te/^{125}Te, and ^{130}Te/^{125}Te ratios.

Based on Rudge *et al.* (2009),[13] a ^{125}Te–^{128}Te double spike that is optimised for mass-dependent isotope analyses and is prepared from highly enriched (but slightly impure) ^{125}Te and ^{128}Te single spikes, should have a ratio of ^{125}Te/^{128}Te $\approx$ 1.08, which is equivalent to ^{125}Te and ^{128}Te proportions of 0.52 and 0.48, respectively, in the double spike (Fig. 1a, *y*-axis).[13] Such a double spike is, furthermore, ideally employed using mixtures that feature ratios of spike-derived Te *versus* natural Te (S/N) of 1.249, which is equivalent to a proportion of spike-derived Te in the spike-sample mixture of approximately 0.6 (Fig. 1a, *x*-axis). A double spike of this composition has an estimated error on the natural mass-fractionation factor (α) of approximately 23 ppm per amu (Fig. 1b).[13] Fig. 1a shows the modelled errors in the natural fractionation factor α for a double spike inversion using the preferred isotope ratios based on the proportion of ^{125}Te in the ^{125}Te–^{128}Te double spike and the proportion of double spike in the double spike – sample mixture. The ideal value is in the center (marked with a red 'X'). Fig. 1b shows the propagation of the uncertainty of the natural fractionation factor α (in ppm per amu) relative to the proportion of the double spike in the double spike – sample mixture.

Whilst there are other double spike combinations available that would produce smaller uncertainties than the chosen double spike composition, these include minor Te isotopes that suffer from large isobaric interferences from Sn (^{120}Te, ^{122}Te, ^{124}Te), Sb (^{123}Te), and Xe (^{124}Te). Although the more abundant Te isotopes have interferences from Xe (^{126}Te, ^{128}Te, and ^{130}Te) and Ba (^{130}Te), except for ^{125}Te which is interference free, the ratios of the interfering isotopes to the affected Te isotopes are much smaller than for the minor Te isotopes, which minimises the analytical uncertainties introduced from the interference corrections.

Highly enriched samples of ^{125}Te (99.76% purity) and ^{128}Te (99.90% purity) were purchased from IsoFlex USA. The enriched isotopes were digested separately in pre-cleaned Savillex PFA vials using a mixture of 15 M HNO_3 and 6.5 M HCl in a ratio of 3 : 1. The solutions were refluxed at 110 °C until the Te was fully dissolved, and subsequently evaporated to incipient dryness. The residues were thereafter dried down three times with 6.5 M HCl to remove any residual HNO_3 and dissolved in 6.5 M HCl.

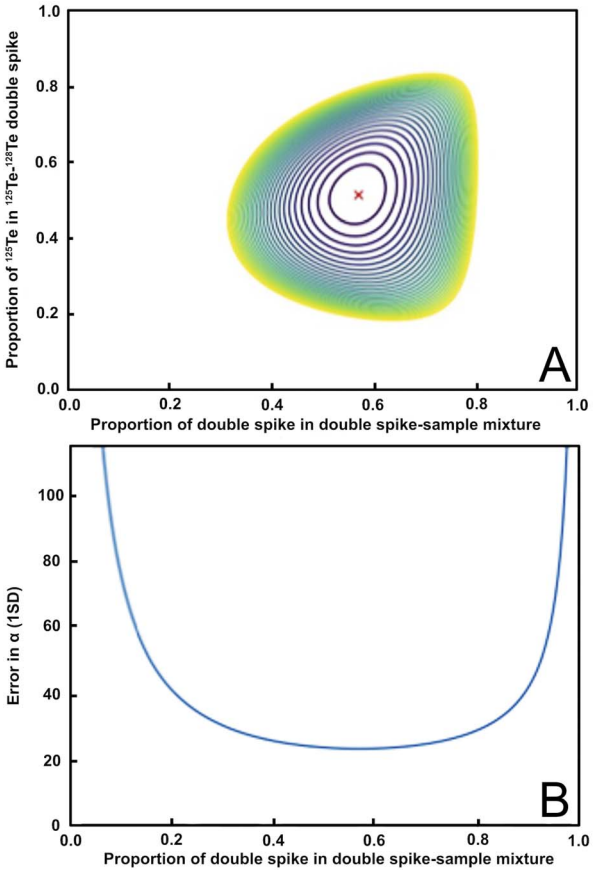

Fig. 1 Panel (A) shows the error in the natural fractionation factor α for the ^{125}Te–^{128}Te double spike composition and inversion isotopes used in this study. The optimal value ratios of ^{125}Te to ^{128}Te (0.52 : 0.48; *y*-axis) and the proportion of double spike in the double spike sample mixture ($\approx$0.6; *x*-axis) are marked by the red 'X'. (B) Shows the propagation of the uncertainty of the natural fractionation factor α in ppm per amu based on the proportion of the ^{125}Te–^{128}Te double spike in the spike-sample mixture. Both plots were produced using the python double spike package 'pyspike' version 1.0.0.[13]

The double spike was then prepared as a mixture of the single spike solutions characterised by ^{125}Te/^{128}Te $\approx$ 1.05. This is equivalent to ^{125}Te and ^{128}Te proportions of about 0.51 and 0.49 in the double spike, respectively, and the use of a ^{125}Te–^{128}Te double spike of this composition allows for accurate determination of mass-dependent Te isotope compositions over a large range of S/N ratios (Fig. 1).

Double spike calibration. The Te concentration of the double spike was determined using reverse isotope dilution relative to the gravimetrically prepared London Te standard solution. In detail, three gravimetric mixtures of the ^{125}Te–^{128}Te double spike and the London Te standard solution were prepared and analysed using instrumental protocols similar to those outlined below. These analyses yielded a Te concentration of 368 ng g^{-1} for the double spike. An initial determination of the double spike isotope composition was carried out by repeated analyses of the 368 ng g^{-1} double spike solution, using a mass bias correction that was determined in previous analyses of the London Te solution, which utilised internal normalisation.

The accuracy of this initial calibration was verified and optimised based on analyses of London Te – double spike mixtures with variable S/N values relative to bracketing measurements of a London Te – double spike reference mixture with the modelled optimal S/N ratio of 1.249.[13] In detail, 14 mixtures with S/N values ranging from 0.09 to 12.6 were analysed during two separate 6 hours measurement sessions. With the optimised double spike calibration, all mixtures except those with S/N $\leq$ 0.46 yielded δ^{130}Te values that were identical, within error ($\pm$0.1‰, 2SD, $n = 30$), to the value obtained for the reference mixture with S/N = 1.249 (Fig. 2).

A S/N value of 2.5 was subsequently adopted as the standard S/N ratio for all further analyses of samples with Te concentration of 100 ng g^{-1} or above. For samples with a Te concentration of less than 100 ng g^{-1}, a S/N ratio of about 3.5 was used to ensure that more total Te was available for the measurements. These S/N ratios were chosen as London Te - double spike mixtures with S/N > 1.7 displayed the best between-run reproducibilities, with a mean of 0.05‰ (2SD, $n = 9$).

Samples and analytical methods

Two meteorites and four terrestrial samples were analysed to characterise the performance of the analytical methods and enable a comparison of results with previously published data. The meteorites analysed in this study are the IAB-complex iron meteorite Canyon Diablo and the CV3 carbonaceous chondrite Allende. The terrestrial samples encompass the Alexo komatiite reference material KAL-1 and three rock reference materials from the USGS, encompassing the ferromanganese (Fe–Mn) nodules, NOD-A-1 and NOD-P-1, and Hawaiian basalt BHVO-2 (Table 6). These samples were chosen as they are either (i) common reference materials (or a widely available meteorite) which were previously characterised in one or more studies (Allende CV3, NOD-A-1, NOD-P-1, BHVO-2) or (ii) previously uncharacterised but widely available samples that are therefore valuable novel additions to the data set (Canyon Diablo, KAL-1).

The sample powder aliquots ranged in mass from 10 to 12 mg for NOD-A-1, 45 to 46 mg for NOD-P-1, 220 to 260 mg for Canyon Diablo, 290 to 320 mg for Allende, and 3.0 to 3.2 g for BHVO-2. A total of 1.43 g of KAL-1 was digested (Table 6). Digested sample masses were chosen based on Te concentrations reported in previous studies (where available), with the aim to provide enough natural Te for several repeat measurements. In the absence of published Te concentrations, the minimum mass required was estimated based on similar samples. In addition to the established reference materials, a glacial till from Greenland and the NIST high-sulphur steel reference material SRM 129c were used to evaluate the impact of molecular and non-spectral interferences on the measured mass-dependent Te isotope composition, as these samples were taken to be representative for terrestrial rocks and meteorites with a silicate mineralogy and iron meteorites, respectively.

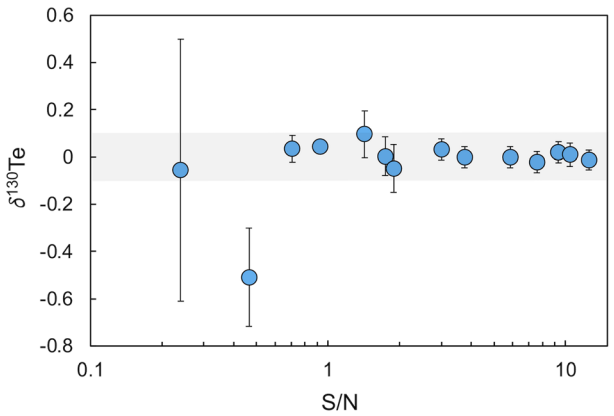

Fig. 2 Plot of δ^{130}Te for mixtures of the Te double spike with the London Te standard solution at varying S/N values. The shaded area denotes the within day precision of 0.1‰ (2SD).

All samples, with the exception of Canyon Diablo, were spiked prior to digestion with appropriate masses of the ^{125}Te–^{128}Te double spike. The glacial till and NIST SRM 129c were additionally doped with 500 ng to 1000 ng of London Te. The digestions were performed in 22 mL or 60 mL Savillex PFA vials. The glacial till, Allende, KAL-1, and BHVO-2 were digested using a three-step digestion protocol adapted from Fehr *et al.* (2004)[10] and Palk *et al.* (2018).[14] In detail, the samples were first treated with a 2.5 + 1 mixture of 28 M HF and 15 M HNO_3 in which they were left for 24 to 48 hours at 110 °C. After evaporation to complete dryness, the samples were taken up in a 1 + 1 mixture of 15 M HNO_3 and 6 M HCl and subsequently refluxed for up to 48 hours at 110 °C. Following this, the samples were evaporated to incipient dryness and subjected to several dry downs using 6 M HCl to ensure complete removal of any remaining HNO_3. Finally, the samples were left to reflux for up to 96 hours in 6 M HCl at 110 °C.

The manganese nodules and NIST SRM 129c were digested using a two-step digestion procedure that encompassed the last two steps of the three-step digestion protocol employed for the glacial till, Allende, KAL-1, and BHVO-2. The Canyon Diablo aliquots analysed in this study were spiked after digestion as they were already digested as part of an earlier study by Poole *et al.* (2017).[15] To ensure full equilibration between sample-derived (natural) Te and spike-derived Te, all samples which were spiked after digestion were evaporated to incipient dryness before being taken up in a 1 + 1 mixture of 15 M HNO_3 and 6 M HCl and refluxed on a hotplate at 120 °C to convert Te to the same oxidation state. The samples were subsequently evaporated to incipient dryness and dried down several times using 6 M HCl to ensure complete removal of any remaining HNO_3 before being taken up in 6 M HCl and refluxed on a hotplate for up to 96 hours.

Column chromatography

A new purification procedure was developed to separate Te from meteorites and terrestrial samples (Table 1). Special attention was directed towards an efficient separation of Te from Fe, Mo, Sn, Zr, Ag, and Cd without unnecessarily lowering the sample yields.

The first step is adapted from the "HCl-protocol" of Fehr *et al.* (2004)[10] and serves to separate Te from the majority of

Table 1 Column chromatography procedure for separation and purification of Te from rocks and meteorites

Eluent	Volume	Purpose/Eluted
Purification step 1: 10 mL BioRad PolyPrep columns with 2 mL BioRad AG1-X-8 resin (200–400 mesh)		
1 M HNO_3	10 mL	Cleaning
2 M HCl	1 mL	Conditioning
2 M HCl	10 mL	Conditioning
2 M HCl (sample)	15 mL	Matrix
2 M HCl	10 mL	Matrix
12 M HCl	6 mL	Ag, Cd
5 M HF	8 mL	Ag, Cd
0.5 M HCl	10 mL	Te
Purification step 2: 3.6 mm × 22.5 mm Teflon microcolumns with 200 μL Eichrom TRUSpec™ resin (100–150 mesh)		
7.5 M HNO_3	10 mL	Cleaning, conditioning
7.5 M HNO_3 (sample)	0.5 mL	Te
7.5 M HNO_3	10 mL	Te
Purification step 3: 10 mL BioRad PolyPrep columns with 2 mL BioRad AG1-X-8 resin (200–400 mesh)		
0.5 M HCl	10 mL	Cleaning, conditioning
0.5 M HCl (sample)	1 mL	Matrix (<1% Te)
0.5 M HCl	10 mL	Te
Purification step 4: 10 mL BioRad PolyPrep columns with 0.4 mL BioRad AG1-X-8 resin (200–400 mesh)		
1 M HNO_3	6 mL	Cleaning
0.5 M HCl	6 mL	Cleaning, conditioning
6 M HCl	4 mL	Conditioning
6 M HCl (sample)	3 mL	Matrix
6 M HCl	5 mL	Matrix
2 M HCl	5 mL	Matrix
0.5 M HCl	10 mL	Te

matrix elements, Ag, Sn, and Cd. This purification step uses 10 mL BioRad Poly-Prep chromatography columns with 2 mL AG1-X-8 anion-exchange resin (200–400 mesh). After cleaning and conditioning of the resin using 10 mL 1 M HNO_3 followed by 10 mL 2 M HCl, the samples were loaded in 15 mL 2 M HCl. The columns were then rinsed with 10 mL 2 M HCl, followed by 6 mL 12 M HCl and 8 mL 5 M HF. Finally, Te was eluted using 10 mL of 0.5 M HCl (Table 1).

The second step is adapted from Hellmann *et al.* (2020)[3] to further purify Te from Mo and Fe. This step uses Teflon microcolumns with resin bed dimensions of 3.6 mm × 22.5 mm loaded with 230 μL Eichrom TRU-Spec resin (100–150 mesh). The resin was cleaned and conditioned using 10 mL 7.5 M HNO_3 before loading the samples in 0.5 mL 7.5 M HNO_3. The Te fractions of the samples were collected immediately upon loading. The resin was then rinsed using 2.5 mL 7.5 M HNO_3 to elute any remaining Te. The total volume of the Te fraction was 3 mL (Table 1).

The collected Te fractions were cleaned by liquid–liquid extraction with *n*-heptane immediately after elution to remove any organic compounds derived from the Eichrom TRU-Spec resin.[16]

The third step further purifies Te from Sn, Ag, and Cd, and was modified from Wang *et al.* (2017)[17] and Wasserman and Johnson (2020).[9] Two mL of AG1-X8 anion-exchange resin (200–400 mesh) was loaded into 10 mL BioRad Poly-Prep chromatography columns and subsequently rinsed using 10 mL 0.5 M HCl to clean and condition the resin. Following this, the samples were loaded onto the resin in 1 mL 0.5 M HCl. The Te was subsequently eluted with 10 mL 0.5 M HCl (Table 1).

Samples with Te contents of <50 ng g^{-1} were processed through an additional purification step to remove residual matrix elements. This fourth step was modified from the protocol of Brennecka *et al.* (2017)[18] and utilises 10 mL BioRad Poly-Prep chromatography columns loaded with 0.4 mL of AG1-X-8 anion-exchange resin (200–400 mesh). The resin was cleaned and conditioned first with 6 mL 1 M HNO_3, followed by 6 mL 0.5 M HCl, and finally 4 mL 6 M HCl. Following this, the samples were loaded in 3 mL 6 M HCl. The columns were subsequently rinsed using 5 mL 6 M HCl followed by 5 mL 2 M HCl. Tellurium was finally eluted with 10 mL 0.5 M HCl (Table 1).

Mass spectrometry

Instrumental parameters. The Te isotope measurements were conducted at the MAGIC Laboratories at Imperial College London with a Nu Instruments Nu Plasma II MC-ICP-MS. Sample introduction was achieved with a Cetac autosampler coupled to a Cetac Aridus II desolvating sample introduction system. A PFA MicroFlow nebuliser with an uptake rate of approximately 140 μL min^{-1} was used. Full details of instrumental operating conditions are summarized in Table 2. The Faraday cup setup, as well as the abundances of Te isotopes and relevant spectral interferences, are shown in Table 3.

The Faraday cups of the Nu Plasma II were fitted with $10^{11}\Omega$ resistors, and the ion beams of ^{129}Xe, and ^{134}Ba (together with isobaric ^{134}Xe) were collected concomitant with ^{125}Te, ^{126}Te, ^{128}Te, and ^{130}Te by static multi-collection during each measurement sequence to allow for corrections of isobaric interferences (Table 3). The analyte solutions were prepared in a mixture of 0.1 M HNO_3 and 0.01 M HF, where the latter was

Table 2 Instrumental operating conditions and protocol for Te isotope measurements

NuPlasma II	
Faraday cup resistors	10^{11} Ω
RF Power	1300 W
Sampler cone	Ni
Skimmer cone	Ni
Coolant airflow	13 min^{-1}
Auxiliary airflow	0.9 min^{-1}
Sample introduction system	**CETAC Aridus II**
Nebulizer	PFA MicroMist pneumatic nebulizer
Nebulizer uptake rate	140 μL min^{-1}
Desolvator temperature	110 °C
Membrane oven	160 °C
Te isotope measurements	
Number of blocks per run	3
Integration time per cycle	5 seconds
Baseline measurement	30 seconds

Table 3 Faraday cup setup detailing the measured Te isotopes and associated isobaric and polyatomic interferences

Cup	H1	H2	H4	H5	H6	H10
Tellurium	^{125}Te	^{126}Te	^{128}Te		^{130}Te	
	7.%	18.8%	31.8%		34.2%	
Isobaric interferences						
Xe		^{126}Xe	^{128}Xe	^{129}Xe$_m$	^{130}Xe	^{134}Xe
		0.09%	1.9%	26.4%	4.1%	10.4%
Ba					^{130}Ba	^{134}Ba[a]
					0.1%	24.4%
Polyatomic interferences						
Nitrides	^{111}Cd	^{112}Cd	^{114}Cd		^{116}Cd	
($+^{14}$N)	12.8%	24.1%	28.7%		7.5%	
		^{112}Sn	^{114}Sn		^{116}Sn	
		1%	0.7%		14.5%	
Oxides	^{109}Ag[b]	^{110}Cd	^{112}Cd		^{114}Cd	
($+^{16}$O, ^{18}O)	48.2%	12.5%	24.1%		28.7%	
	^{107}Ag[c]	^{110}Pd	^{112}Sn		^{114}Sn	
	51.8%	11.7%	1%		0.7%	
Argides	^{85}Rb	^{86}Kr	^{88}Sr		^{90}Zr	
($+^{40}$Ar)	72.2%	17.3%	82.6%		51.5%	
		^{86}Sr				
		9.9%				

[a] Monitor isotope used for isobaric interference corrections. [b] ^{16}O. [c] ^{18}O.

added to avoid Te precipitation during storage and in the sample introduction system. Typical total Te concentrations for the analyte solutions ranged between 20 ng mL^{-1} and 30 ng mL^{-1}.

The sensitivity for Te was influenced by the instrumental setup and tuning parameters, which were optimised prior to each measurement session. The typical sensitivity was 750 V (μg^{-1} mL^{-1}) during the course of the study, which is equivalent to a transmission efficiency of 0.50%.

The isotope ratio measurements were carried out in three blocks of 20 cycles, with an integration time of 5 s each. Each block was preceded by a 30 s electronic baseline measurement during which the ion beam was deflected by the electrostatic analyser. The system was flushed between analyses with a mixture of 0.1 M HNO_3 and 0.01 M HF. The time required for one measurement, including the wash-out sequence, was about 10 minutes (Table 2). All sample analyses were bracketed by runs of a double-spiked London Te standard solution which was matched to the sample solutions in both concentration and S/N values to within 10%. The Te isotope data reported in this study are expressed relative to the results obtained for multiple runs of the London Te standard during the same measurement session.

Data reduction and isobaric interferences. This study applied an iterative procedure that was carried out offline after completion of the mass spectrometric analyses to determine the mass-dependent Te isotope composition of the samples. The procedure corrects for laboratory-induced and instrumental mass bias as well as isobaric interferences. The procedure was applied to all relevant Te isotopes, as well as the Ba monitor isotope (^{134}Ba). To this end, the data reduction employs the isotope ratios ^{126}Te/^{125}Te, ^{128}Te/^{125}Te and ^{130}Te/^{125}Te, with ^{125}Te chosen as the denominator as it is the only Te isotope free from isobaric interferences. The other Te isotopes exhibit isobaric interferences from Xe (^{126}Te, ^{128}Te, and ^{130}Te) and Ba (^{130}Te). The Xe interferences on ^{126}Te, ^{128}Te, ^{130}Te, and ^{134}Ba were monitored using ^{129}Xe and corrected using Xe isotope ratios of ^{126}Xe/^{129}Xe = 0.00337, ^{128}Xe/^{129}Xe = 0.07235, ^{130}Xe/^{129}Xe = 0.15420, and ^{134}Xe/^{129}Xe = 0.39528.[19]

The Ba interference on ^{130}Te was monitored using ^{134}Ba, which was corrected for the interference of ^{134}Xe prior to use. The Xe-corrected ^{134}Ba ion beam was then applied to correct the Ba interference on ^{130}Te using a Ba isotope ratio of ^{130}Ba/^{134}Ba = 0.04386.[19] However, as the large Xe corrections on ^{134}Ba often resulted in a nominally negative ^{134}Ba ion beam intensity, the Ba interference correction was only applied if the Xe-corrected ^{134}Ba ion beam was ≥0 mV.

All Te concentrations reported in this study were determined by isotope dilution. The technique is employed here using the measured and mass-bias corrected ^{125}Te/^{130}Te and ^{128}Te/^{130}Te ratios of the double spike sample solutions. The data necessary for the calculation of the Te concentration of a sample were obtained during the runs that were carried out to determine the stable isotope compositions. Due to this, the number of measurements (n) given for a sample in Tables 6 and 7 applies both to the Te isotope composition and the Te concentration.

Results and discussion

Yields and blanks

The yields of the column chemistry procedure for the separation of Te were determined by passing known quantities of the London Te standard solution through the columns and subsequent collection of all eluate fractions after the 'sample' had been loaded. The total beam intensity – calculated from monitoring ^{125}Te, ^{126}Te, ^{128}Te, and ^{130}Te ion beam intensities – were then measured for the 'sample' relative to a London Te standard solution of known concentration, to determine the Te mass recovered for the former.

The full procedural yields ranged from 85% to 95%. Stage 1 of the column chemistry achieved yields of 90% to 95%, whilst near-quantitative yields of 97% to 100% were obtained for stages 2, 3, and 4 of the Te separation.

Excluding one outlier, the total Te blank of the analytical procedure ranged from 34 pg to 77 pg, with a mean of 54 ± 15 pg (1SD, n = 7). The single high-Te outlier blank was measured at 390 pg. The measured Te concentrations were corrected for the contribution of the blank. No blank corrections were applied to the Te isotope compositions of samples as the typical blank contributed ≤0.01‰ to the total natural Te analysed and the Te isotope composition of the blank is not well defined.

Evaluation of spectral and non-spectral interferences

Measurements of Te isotopes by MC-ICP-MS can be affected by spectral interferences from isobars and polyatomic ions as well

as the presence of elements that can generate non-spectral interferences (*i.e.*, matrix effects).

Isobaric interferences. The Xe/Te ratios of the samples in this study ranged from 1.8×10^{-3} to 9.7×10^{-3}, which is nearly indistinguishable from the Xe/Te ratios of the London Te standard solution – double spike mixtures, which ranged from 1.7×10^{-3} to 9.6×10^{-3}. At this level, the isobaric interferences from Xe had no significant impact on the measured Te isotope compositions and the within-session precision of the data.

The Xe-corrected ion beam intensity of ^{134}Ba was <0 mV for most samples, and hence Ba-corrections were not commonly applied. When the amount of Ba present was large enough for a Ba correction to be applied, the Ba/Te ratios ranged from 1.6×10^{-5} to 1.7×10^{-4}, with a mean of 9.6×10^{-5}. At this level, the Ba/Te ratios had no significant effect on the within-day precision nor the measured δ^{130}Te values.

Molecular and non-spectral interferences. Problematic polyatomic interferences can arise from diatomic molecules of ^{14}N, ^{16}O, ^{18}O, and ^{40}Ar with Rb, Sr, Zr, Ag, Cd, and Sn, as well as hydrides that may form with Te, I and Xe (Table 3). Additionally, it has been reported that Fe in sample solutions may induce matrix effects that can bias Te isotope measurements.[10]

The impact of Rb, Sr, Zr, Ag, Cd, and Sn on the Te isotope analyses was evaluated through repeat analyses of the glacial till and NIST SRM 129c. In addition, appropriate aliquots of the final Te fractions from the column chemistry were analysed using mass scans for the presence of Fe, Rb, Sr, Zr, Ag, Cd and Sn. The ion beam intensities measured for these elements were then compared to the Te ion currents obtained for the same solutions in order to quantify acceptable Element/Te levels, which are not associated with any impacts on the measured Te isotope compositions.

The Sn/Te ratios of the samples ranged from 1.5×10^{-4} to 8.9×10^{-4}, with a mean of 2.3×10^{-4}. This is nearly identical to the Sn/Te ratios of the London Te standard solution-double spike mixtures which ranged from 1.5×10^{-4} to 5.7×10^{-4}. Occasionally, higher Sn/Te ratios of up to 2.9×10^{-3} were measured for some samples. Regardless, even at this higher level, Sn had no influence on measured δ^{130}Te values and the reproducibility of the data.

Strontium was found to have similarly negligible effect on the Te isotope data, even at Sr/Te ratios of up to 0.87, which is significantly higher than the Sr/Te levels of <0.13 specified by Fehr *et al.* (2004).[10]

The Zr/Te ratio of the samples ranged from 1.2×10^{-3} to 1.5×10^{-3}, whilst the Element/Te levels of Rb, Ag, and Cd did not exceed 0.05 for any of the samples. At these levels, neither Zr, Rb, Ag, or Cd had a noticeable effect on the measured δ^{130}Te values or the reproducibility of the data.

Finally, the Fe/Te ratios of the samples ranged from 0.11 to 0.20, with a mean of about 0.16. At this level the Fe present in the samples had no effect on the measured δ^{130}Te values nor the reproducibility of the data, indicating that the Te isotope compositions presented here are unlikely to have been affected by matrix effects from Fe.

While the production rates of hydrides of Te, I, and Xe in the plasma are expected to be limited due to the use of a desolvating nebuliser system for sample introduction, their presence may still affect the Te isotope compositions. As such, the production rates of these hydrides were evaluated to determine their potential impact (if any) on measured δ^{130}Te values. Given that I and Xe are trace constituents of the plasma gas, hydrides of these elements are expected to generate constant interference levels, and their presence should hence be detectable from variations in Te isotope ratios when Te is present at different concentrations. To investigate this, pure Te standard solutions with concentrations ranging from 50 ng mL^{-1} to 200 ng mL^{-1} were analysed against a primary standard with a Te concentration of 100 ng mL^{-1} in five separate 6- to 8-hours measurement sessions over a period of ten months. No significant deviations in isotopic composition between Te solutions of different concentrations were found in any of the sessions. This demonstrates that problematic levels of IH^+ and XeH^+ were not present during the analyses due to limited hydride formation. The production of TeH+ was monitored based on variations in ion beam intensities as mass number 129 (^{129}Xe), and the upper limit of ^{128}TeH+/^{128}Te was found to be <5 ppm. This suggest that TeH+ formation in the plasma is essentially negligible and does not compromise the δ^{130}Te values reported here.

Potential impact of mass-independent Te isotope effects

The double spike data reduction assumes that any isotopic variations identified for samples are due to mass-dependent isotope fractionation. However, if the isotope composition of a sample is also altered by radiogenic decay, material of distinct nucleosynthetic origin, or mass-independent isotope fractionation, the data reduction will yield biased mass-dependent isotopic compositions and hence incorrect δ-values. For samples that harbour such isotope anomalies, the issue can be addressed by carrying out additional analyses of the unspiked sample and application of this isotope data in the double spike data reduction.[13,20]

In order to investigate the impact of potential mass-independent isotope effects on mass-dependent Te isotope compositions, the current study calculated the maximum mass-independent isotope anomalies that can be tolerated for a sample before this has a deleterious impact on the measured δ^{130}Te values.[20]

Nucleosynthetic and radiogenic Te isotope anomalies and mass-independent Te isotope fractionations have yet to be unambiguously identified in natural samples.[2,3,18,21–23] The following calculations therefore employed a theoretical sample, which was assigned nucleosynthetic anomalies on the ^{126}Te/^{125}Te, ^{128}Te/^{125}Te and ^{130}Te/^{125}Te ratios and that correspond to anomalies that would be expected for a small deficit of isotopes produced by s-process nucleosynthesis.

The isotopic anomalies are quantified with the ε-notation, which denotes the relative deviation of an isotope ratio determined for a sample from the value measured for a standard reference material in parts per 10 000. For the modelling, the Te isotope anomalies were scaled to be just larger than the analytical errors that were reported in previous studies for measurements of ε^{126}Te, as scaling the anomalies relative to the

analytical errors reported for ε^{130}Te would result in ε^{126}Te anomalies of ≥1.4, which are significantly larger than those reported in any previous studies.[3,21,22] The calculations summarized above yield maximum mass-independent Te isotope anomalies of $\varepsilon^{126}\text{Te} = -0.43$ and $\varepsilon^{130}\text{Te} = -0.17$. If such anomalies were present in a sample, they would generate a shift in δ^{130}Te of only ±0.025‰. Importantly, such a small shift cannot be resolved analytically as it much smaller than the typical within-session reproducibility of ±0.07‰ (2SD) that was obtained in this study for δ^{130}Te measurements.

An additional isotope effect of $\varepsilon^{126}\text{Te} = +0.1$ was also incorporated to account for possible additional radiogenic ingrowth of ^{126}Te from decay of extinct ^{126}Sn in meteorites. This addition resulted in a revised mass-independent Te isotope anomaly of $\varepsilon^{126}\text{Te} = -0.33$. Applying the updated mass-independent Te isotope anomalies of $\varepsilon^{126}\text{Te} = -0.33$ and $\varepsilon^{130}\text{Te} = -0.17$ reduced the shift in δ^{130}Te to ±0.022‰. As such, possible radiogenic and nucleosynthetic Te isotope effects in meteorites and terrestrial samples are unlikely to have a significant impact on δ^{130}Te values.

In addition to nucleosynthetic and radiogenic anomalies, anomalous Te isotope effects can be introduced to a sample due the nuclear field shift effect (NFSE).[24–26] Isotope fractionations consistent with NFSEs have been reported for Te during solvent extraction experiments.[24] The NFSE is generally accepted to occur concurrently with mass-dependent isotope fractionation and is thought to be a significant source of isotope fractionation for the heaviest elements, including Hg, Tl and U.[24–27] Consequently, while the behaviour in lighter elements is poorly constrained, NFSEs could be a significant contributor to Te isotope fractionation.

As direct investigations are hampered by the lack of NFSE data for Te, this study calculated an upper constraint on the impact of the NFSE. This was done by numerically adding mass-independent anomalies to the isotopic composition of the London Te standard solution, processing these results through the double spike data reduction, and subsequently calculating the difference in mass-dependent isotope composition between the hypothetical dataset and the standard.[26] The mass-independent anomalies were calculated in ε-units using eqn (1) from Fujii *et al.* (2006):[26]

$$\varepsilon^{i}\text{Te} = \left[\delta\left(r^2\right)_{m_{126},\, m_i} - \frac{m_{130}(m_i - m_{126})}{m_i(m_{130} - m_{126})}\delta\left(r^2\right)_{m_{126},\, m_{130}}\right] \times \alpha \quad (5)$$

The equation is presented here using the example of ε^{i}Te normalised to $^{130}\text{Te}/^{126}\text{Te} = 1.81684$.[25] Here m_i is the atomic weight of the nuclide '*i*' in ε^{i}Te, m_{130}, m_{126}, are the atomic weights of the nuclides in the normalisation ratio (^{130}Te, ^{126}Te), and $\delta(r^2)$ is the squared change in the nuclear charge radii of the nuclei. The variable α is an adjustable parameter which is determined through regression.[27–29]

The above calculations, when scaled according to the maximum analytical errors that were reported in previous studies and which did not observe NFSE, yielded a maximum mass-independent anomaly of $\varepsilon^{128}\text{Te} = -0.91$.[21–23] Anomalies of this magnitude would contribute a maximum of ±0.037‰ to the mass-dependent δ^{130}Te values, which is significantly less than the typical within-session reproducibility of ±0.07‰ (2SD) that was obtained in this study for δ^{130}Te measurements. If the calculations are instead performed using data normalised to $^{125}\text{Te}/^{128}\text{Te} = 0.22204$, this results in mass-independent Te isotope anomalies of $\varepsilon^{126}\text{Te} = -0.30$ and $\varepsilon^{130}\text{Te} = +0.30$.[30] Anomalies of this magnitude would generate a shift in δ^{130}Te of ±0.080‰ and could hence result in an analytically just resolvable shift for δ^{130}Te.

In summary, the calculations indicate that mass-independent Te isotope anomalies from radiogenic decay, distinct nucleosynthetic matter, and NFSE are expected to have either no or only a barely resolvable impact on the measured δ^{130}Te of samples. This reflects that such anomalies are expected to be small because they were previously not clearly resolved in mass-independent Te isotope analyses of terrestrial and meteorite samples.

Analyses of London Te solutions

The precision obtained in repeated analyses of London Te standard solutions was evaluated over a 19 months period, from July 2020 to January 2022. During this time, 18 measurement sessions of about 8 to 16 hours each, were carried out. Each session encompassed about 50 to 100 Te isotope runs and of these about 25 to 60 were analyses of London Te – double spike mixtures. These London Te – double spike mixtures were characterised by S/N ≈ 2.45 and total Te concentration of 25 to 30 ng mL^{-1}, with each run consuming about 30 to 40 ng of Te, equivalent to 8.5 to 11.5 ng of natural Te. For single measurement sessions, these analyses typically yielded a within-session reproducibility (2SD) of ±0.04‰ to ±0.08‰ with a mean of ±0.07‰ (2SD). For individual runs, the typical within-run reproducibility (2SE) ranged from ±0.03‰ to ±0.05‰, with a mean of ±0.04‰. Three additional measurement sessions of about 4 to 6 hours each were performed using London Te – double spike mixtures with total Te concentrations of 15 to 20 ng mL^{-1} and S/N ≈ 2.45. These sessions encompassed 25 to 40 isotope runs of London Te – double spike mixtures. Each run consumed about 18 to 24 ng of total Te, equivalent to 6 to 7.5 ng of natural Te. These analyses typically yielded a within-day reproducibility (2SD) of 0.05‰ to 0.09‰ with a mean of 0.07‰. For individual runs, the typical within-run reproducibility (2SE) ranged from 0.05‰ to 0.06‰, with a mean of 0.05‰.

Analyses of secondary Te isotope reference materials. Analyses of three secondary Te standard solutions were carried out routinely alongside samples during each measurement session. Such analyses utilised mixtures of the secondary standard solutions with the Te double spike and which featured S/N ratios of 2.5 to 2.7 and total Te concentration of about 25 ng mL^{-1}. These analyses yielded a combined mean δ^{130}Te values of 0.93 ± 0.06‰ for AA-ETH Te (2SD, $n = 73$), 0.81 ± 0.05‰ for NIST-ETH Te (2SD, $n = 93$), and 0.44 ± 0.05‰ for NIST-Münster Te (2SD, $n = 17$) relative to London Te (Table 4).

All secondary Te standard solutions used here were thoroughly characterised in previous studies and they can,

Table 4 δ^{130}Te values determined for secondary Te isotope reference materials relative to London Te

Te standard solution	n	δ^{130}Te (±2SD)
AA-ETH Te	73	0.93 ± 0.06‰
NIST-ETH Te	93	0.81 ± 0.05‰
NIST-Münster Te	17	0.44 ± 0.05‰

therefore, be used to verify that the new protocols developed here provide unbiased δ^{130}Te data.[2–4] In detail, the results of this study yield a δ^{130}Te of −0.12 ± 0.06‰ for NIST-ETH Te relative to the AA-ETH Te, which is identical to the offset of −0.12 ± 0.03‰ reported by Fehr *et al.* (2018)[2] (Table 5).

Furthermore, NIST-ETH Te and AA-ETH Te have positive δ^{130}Te values, of 0.37 ± 0.04‰ and 0.49 ± 0.05‰, respectively, relative to NIST-Münster Te (Table 5). To enable a direct comparison of these data with the previous results of Hellmann *et al.* (2021),[4] the latter data were recalculated from $\delta^{128/126}$Te to δ^{130}Te notation using eqn (2) (Table 5).

Based on these calculations, the data of Hellmann *et al.* (2021)[4] yield δ^{130}Te values for NIST-Münster Te relative to NIST-ETH Te and AA-ETH Te of −0.37 ± 0.07‰ and −0.50 ± 0.05‰, respectively, and these are both identical to the results of this study (Table 5).

Tellurium concentrations of meteorites and terrestrial samples

Repeat analyses of a single digestion of komatiite KAL-1 yielded a mean Te concentration of 35.6 ± 0.1 ng g^{-1} (1SD, n = 4). As KAL-1 has not previously been analysed for its Te concentration, a direct comparison to published results is not possible. However, the Te concentration determined for KAL-1 is in line with Te concentrations of 24 ng g^{-1} to 53 ng g^{-1} obtained in three previous studies for the IAG komatiite reference material OKUM.[31–33]

The Hawaiian basalt BHVO-2 displays the lowest Te concentration of the samples analysed in this study, with a combined mean of 14.5 ± 0.4 ng g^{-1} for three different digestions (1SD, n = 3). This is broadly consistent with the Te concentrations of 11.9 ± 1.4 ng g^{-1} to 14.6 ± 2.7 ng g^{-1} reported in seven previous studies (Table 6).[3,34–39]

The Fe–Mn nodule NOD-A-1 has the highest Te concentration of the samples analysed in this study, with a mean of 34.7 ± 0.4 μg g^{-1} (1SD, n = 3). This result is higher than the concentrations of 30.9 ± 0.1 μg g^{-1} and 29.6 ± 0.7 μg g^{-1} that were published by Axelsson *et al.* (2002)[40] and Hellmann *et al.* (2020),[3] respectively. This discrepancy most likely reflects minor sample heterogeneity as Te concentrations ranging from 28.8 μg g^{-1} to 36.0 μg g^{-1} were reported for different sample powder aliquots analysed in the same laboratory.[8] Notably, the imprecise mean value of 32.4 ± 6.5 μg g^{-1} determined by Fukami *et al.* (2018)[8] is consistent with the result of the current study.

The second analysed Fe–Mn nodule, NOD-P-1, has a Te concentration of 5.1 ± 0.0 μg g^{-1} (1SD, n = 3), in line with the results of five previous studies which range from 4.8 ± 0.4 μg g^{-1} to 5.1 ± 0.3 μg g^{-1} (Table 6).[3,8,9,39,41]

Considering the meteorites, replicate analyses of four separate digestions of the CV3 chondrite Allende yielded a mean Te concentration of 970 ± 60 ng g^{-1} (1SD, n = 4), consistent with literature data of 850 ± 140 ng g^{-1} and 940 ± 30 ng g^{-1} (Table 6).[2,3] The mean Te concentration of 122 ± 2 ng g^{-1} (1SD, n = 4) obtained in this study for Canyon Diablo is intermediate to two previous results of 176 ± 20 ng g^{-1} and 90 ± 16 ng g^{-1} (Table 6).[21,41] The observed variability is most likely due to heterogenous distribution of troilite nodules within the Canyon Diablo meteorite as the sulphides are presumably the main carrier phase of Te in iron meteorites.

Tellurium isotope compositions of terrestrial samples

Tellurium isotope data were acquired for four terrestrial samples, Alexo komatiite KAL-1, Hawaiian basalt BHVO-2, and the Fe–Mn nodules NOD-A-1 and NOD-P-1.

Komatiite KAL-1 displays the lightest isotope composition of the terrestrial samples analysed in this study with a mean δ^{130}Te

Table 5 δ^{130}Te values of the Te isotope reference materials expressed relative to each other

This study			
NIST-ETH Te relative to	NIST-ETH Te —	AA-ETH Te −0.12 ± 0.06‰	NIST-Münster Te 0.37 ± 0.05‰
AA-ETH Te relative to	NIST-ETH Te 0.12 ± 0.06‰	AA-ETH Te —	NIST-Münster Te 0.49 ± 0.04‰
NIST-Münster Te relative to	NIST-ETH Te −0.37 ± 0.05‰	AA-ETH Te −0.49 ± 0.04‰	NIST-Münster Te —
Previous studies			
Fehr *et al.* (2018)[2]			
NIST-ETH Te relative to	AA-ETH Te −0.12 ± 0.03‰		
Hellmann *et al.* (2021)[4]			
[a]NIST-ETH Te relative to	NIST-Münster Te 0.37 ± 0.07‰		
[a]AA-ETH Te relative to	NIST-Münster Te 0.50 ± 0.05‰		

[a] Recalculated from $\delta^{128/126}$Te using eqn (2)

Table 6 Te isotope compositions and concentrations of terrestrial samples[a]

	Mass (mg)	δ^{130}Te (±2SD)	n	Te (±1SD)
KAL-1 (Alexo komatiite)				**ng g^{-1}**
Digestion 1	1430	0.64 ± 0.06	4	35.60 ± 0.01
BHVO-2 (Basalt)				**ng g^{-1}**
Digestion 1	3035	1.13 ± 0.07	4	14.00 ± 0.01
Digestion 2	3175	1.15 ± 0.06	4	15.00 ± 0.01
Digestion 3	2950	1.15 ± 0.09	4	14.50 ± 0.01
Mean BHVO-2		**1.14 ± 0.01**	**3**	**14.50 ± 0.41**
[b]**Previous studies**				
Hellmann *et al.* (2020)[3]		1.06 ± 0.08	5	14.5 ± 0.6
NOD-A-1 (Fe–Mn nodule)				**μg g^{-1}**
Digestion 1	12	1.59 ± 0.05	7	34.51 ± 0.02
Digestion 2	10	1.64 ± 0.06	9	34.75 ± 0.16
Digestion 3	10	1.67 ± 0.07	7	34.79 ± 0.03
Mean NOD-A-1		**1.63 ± 0.07**	**3**	**34.74 ± 0.38**
[b]**Previous studies**				
Fehr *et al.* (2018)[2]		1.67 ± 0.08	3	n.d.
Fukami *et al.* (2018)[8]		1.56 ± 0.10	5	32.4 ± 6.5
Hellmann *et al.* (2020)[3]		1.53 ± 0.10	5	29.6 ± 0.7
NOD-P-1 (Fe–Mn nodule)				**μg g^{-1}**
Digestion 1	45	1.43 ± 0.05	5	5.06 ± 0.01
Digestion 2	46	1.34 ± 0.08	5	5.08 ± 0.01
Digestion 3	45	1.40 ± 0.07	4	5.10 ± 0.01
Mean NOD-P-1		**1.39 ± 0.07**	**3**	**5.08 ± 0.03**
[b]**Previous studies**				
Fehr *et al.* (2018)[2]		1.35 ± 0.14	6	n.d.
Fukami *et al.* (2018)[8]		1.12 ± 0.07	5	5.32 ± 0.26
Hellmann *et al.* (2020)[3]		1.22 ± 0.07	5	4.95 ± 0.05
Wassermann and Johnson (2020)[9]		1.08 ± 0.17	5	4.88 ± 0.75

[a] Sample mass in processed sample solution aliquot. [b] Recalculated using offsets detailed in Table 4. Errors were propagated using: $2SD_{final} = \sqrt{((A_{2SD}^2) + (B_{2SD}^2))}$.

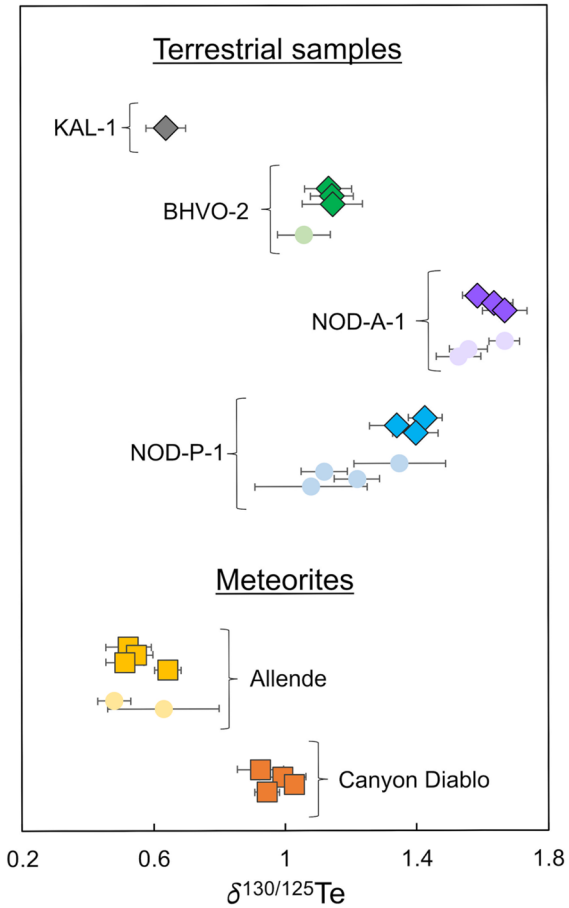

Fig. 3 Plot showing the δ^{130}Te values obtained in this and previous studies. Data obtained in this study are shown as diamonds and squares. Literature data is shown as circles.[2,3,8,9,21] All data are compiled in Tables 6 and 7.

value of 0.64 ± 0.06‰ (2SD, n = 4) obtained from repeat analyses of one digested powder aliquot (Fig. 3 and Table 6).

While no other komatiites have been analysed for the Te isotope compositions to date, the result resembles mass-dependent Te isotope data reported for lherzolites, harzburgites, and dunites in a previous study, which ranged from 0.44 ± 0.05‰ to 0.71 ± 0.054.[4]

Repeat analyses of three separate digestions of BHVO-2 produced a combined mean δ^{130}Te value of 1.14 ± 0.01‰ (2SD, n = 3; Table 6). This is consistent with the previously reported δ^{130}Te value of 1.06 ± 0.08‰ (Fig. 3 and Table 6).[3]

Three separate digestions of nodule NOD-A-1 produced a mean δ^{130}Te value of 1.63 ± 0.07‰ (2SD, n = 3; Table 6). This is in accord with previously reported δ^{130}Te values, which range from 1.53 ± 0.10‰ to 1.67 ± 0.08‰ (Fig. 3 and Table 6).[2,3,8]

The isotope composition of NOD-P-1 is slightly lighter than NOD-A-1, with a mean δ^{130}Te value of 1.39 ± 0.07‰ (2SD, n = 3) from three separate digestions (Table 6). This result is consistent with the δ^{130}Te of 1.35 ± 0.14‰ obtained by Fehr *et al.* (2018),[2] but heavier than the Te isotope compositions of three other studies which reported δ^{130}Te values which ranged from 1.08 ± 0.17‰ to 1.22 ± 0.07‰ (Fig. 3 and Table 6).[3,8,9] This variability is further confirmed by reports of variable δ^{130}Te values for different powder aliquots of this sample that were analysed in the same laboratory.[2,9] Together, this indicates that the NOD-P-1 reference material exhibits significant heterogeneity, as previously suggested by Fukami *et al.* (2018)[8] and Wasserman and Johnson (2020).[9]

Tellurium isotope compositions of meteorites

Repeat analyses of four separate digestions of the CV3 chondrite Allende during the course of this study yielded a mean δ^{130}Te value of 0.56 ± 0.10‰ (2SD, n = 4; Table 7). This result is consistent with δ^{130}Te values of 0.63 ± 0.18‰ and 0.48 ± 0.05‰ from two previous studies (Fig. 3 and Table 7).[2,3] Of interest is the observation that whilst Allende digestions 1, 2, and 3 yielded very consistent δ^{130}Te values of 0.52 ± 0.07‰ (2SD, n = 4), 0.55 ± 0.05‰ (2SD, n = 8), and 0.51 ± 0.06‰ (2SD, n = 12), respectively, digestion 4 provided a higher δ^{130}Te of 0.64 ±

Table 7 Te isotope compositions and concentrations of meteorite samples

	Mass (mg)	δ^{130}Te[a] (±2SD)	n	Te[b] (±1SD)
Allende (CV3 chondrite)				**ng g^{-1}**
Digestion 1	285	0.52 ± 0.07	4	1070 ± 0.7
Digestion 2	320	0.55 ± 0.05	8	935 ± 1.6
Digestion 3	310	0.51 ± 0.06	12	940 ± 1.3
Digestion 4	310	0.64 ± 0.04	10	940 ± 1.7
Mean Allende		**0.56 ± 0.10**	**4**	**970 ± 60**
[c]**Previous studies**				
Fehr *et al.* (2018)[2]		0.63 ± 0.17	3	850 ± 140
[d]Hellmann *et al.* (2020)[3]		0.48 ± 0.05	2	940 ± 30
Canyon Diablo (IAB-complex iron meteorite)				**ng g^{-1}**
Aliquot 1	220[f]	0.92 ± 0.07	1	120
Aliquot 2	220[f]	0.99 ± 0.07	1	121
Aliquot 3	260[f]	1.03 ± 0.02	2	124 ± 0.01
Aliquot 4	250[f]	0.95 ± 0.04	3	124 ± 0.02
Mean Canyon Diablo		**0.97 ± 0.08**	**4**	**122 ± 3**
Previous studies				
[e]Goles and Anders, (1962)[42]		N/A	1	90 ± 16
[c]Fehr *et al.* (2005)[21]		−1.31 ± 2.25	4	176 ± 20

[a] In case of single analyses, the within-session precision is used as sample 2SD. [b] Errors for single analyses are less than 0.001 ng g^{-1} and are not shown. [c] Recalculated using offsets detailed in Table 4. Errors were propagated using: $2SD_{final} = \sqrt{((A_{2SD}{}^2) + (B_{2SD}{}^2))}$. [d] Average of two reported values. [e] The study did not determine the Te isotope composition. [f] Sample mass in processed sample solution aliquot.

0.04‰ (2SD, n = 10; Table 7). This occurred even though all digestions were sourced from a single larger homogenised powdered sample of Allende. Furthermore, digestion 4 was processed and analysed alongside digestions 2 and 3, such that the distinctly heavier Te isotope composition is unlikely to be an analytical artefact from sample preparation or the mass spectrometric analyses. Similar variations in the mass-dependent Te isotope composition of Allende were previously described by Fehr *et al.* (2018),[2] who reported a mean δ^{130}Te of 0.63 ± 0.18‰ for three digestions of the meteorite (Table 7). No such variations were found by Hellmann *et al.* (2020),[3] who obtained a mean δ^{130}Te of 0.48 ± 0.05‰ from two Allende digestions (Fig. 3 and Table 7).

Fehr *et al.* (2018)[2] suggested that the variable δ^{130}Te values they determined for Allende may result from re-distribution of Te during thermal metamorphism. It's unclear, however, whether the weak thermal processing that overprinted Allende was sufficient to mobilise Te and affect its isotope composition on a bulk sample scale.[3,43] Conversely, Hellmann *et al.* (2020)[3] suggested that the bulk compositions of carbonaceous chondrites most likely reflect mixing of a volatile depleted chondrule component with isotopically light Te and a volatile-rich matrix component with isotopically heavy Te. The δ^{130}Te variations found in this study and by Fehr *et al.* (2018)[2] for Allende may, therefore, reflect variable amounts of matrix and chondrule components in the separate digestions. Notably, this interpretation predicts correlated variations of Te isotope compositions and concentrations, but no such correlation is evident for the Allende data of this study and Fehr *et al.* (2018).[2] Alternatively, it is possible that the variable δ^{130}Te data for Allende may result from the heterogenous distribution of one or several phases or components with distinct Te isotope composition, such as sulphides or CAIs, as was previously suggested by Fehr *et al.* (2018).[2] The latter explanation, possibly in combination with variable amounts of matrix and chondrule components, can account for the observed decoupled variations of δ^{130}Te values and Te concentrations in different power aliquots of the Allende meteorite.

The four solution aliquots of the IAB complex iron meteorite Canyon Diablo that were analysed in this study yielded a combined mean δ^{130}Te of 0.97 ± 0.08‰ (2SD, n = 4; Table 7 and Fig. 3). Notably, this is the first precise mass-dependent Te isotope composition determined with the double spike technique for any iron meteorite. The only previously available mass-dependent Te isotope data for iron meteorites had much larger errors, of up to ±0.9‰ for $\delta^{126/128}$Te, as they were obtained without use of a double spike or dopant element for correction of the instrumental mass bias. Furthermore, the δTe = 0 reference material that was employed by Fehr *et al.* (2005)[21] has not been analysed relative to the primary Te isotope reference materials that were used in this and other recent studies. However, assuming no isotopic offset between the δTe = 0 reference material of Fehr *et al.* (2005)[21] and the London Te of this study, the combined mean $\delta^{126/128}$Te value of 0.53 ± 0.90‰ reported for Canyon Diablo by Fehr *et al.* (2005)[21] is equivalent to a δ^{130}Te value of −1.3 ± 2.25‰. Within error, this overlaps with the δ^{130}Te value of 0.97 ± 0.08‰ obtained in this study, such that the results can tentatively be assumed as consistent (Table 7).

Conclusions

This study presents new methods for the precise determination of mass-dependent Te isotope compositions. In particular, the technique encompasses a new protocol for the separation of Te from silicate rock and meteorite samples as well as iron meteorites prior to the isotopic analyses. The separation method efficiently isolates Te from elements that produce spectral and non-spectral interferences during the measurements whilst providing yields of >85%. The method employs a ^{125}Te–^{128}Te double spike, which provides a robust correction for any mass-bias effects that are incurred during sample preparation and the MC-ICP-MS analyses.

In an 8-to-12-hours measurement session the typical between-run reproducibility (2SD) of the δ^{130}Te data is ±0.07‰, for analyte solutions with Te concentrations of 20 ng mL^{-1} to 30 ng mL^{-1} and runs that each consume 30 to 40 ng Te. This is on par with, or better than, the precisions achieved in other recent Te isotope studies.

The methods were validated based on an inter-laboratory cross-calibration of three different Te standard solutions and analyses of three rock reference material and two meteorites for which Te concentrations and isotope compositions were available in the literature. In detail, the δ^{130}Te values determined in this study for AA-ETH Te relative to NIST-ETH Te (−0.12 ±

0.06‰) and for NIST-Münster Te relative to NIST-ETH Te and AA-ETH Te (−0.37 ± 0.04‰ and −0.49 ± 0.05‰, respectively) are identical to the results of previous investigations. Combined, this shows that the δ^{130}Te values obtained in this study are unbiassed.

This study reports δ^{130}Te values for four previously investigated samples; three terrestrial reference samples and the CV3 carbonaceous chondrite Allende. The terrestrial samples include Hawaiian basalt BHVO-2 and Fe–Mn nodules NOD-A-1 and NOD-P-1, which display δ^{130}Te values of 1.14 ± 0.01‰, 1.63 ± 0.07‰, and 1.39 ± 0.07‰, respectively. Type 3 CV chondrite Allende has a δ^{130}Te value of 0.56 ± 0.10‰. Tellurium concentrations were obtained for all four samples *via* isotope dilution, where BHVO-2, NOD-A-1, NOD-P-1, and Allende display mean Te concentrations of 14.5 ± 0.1 ng g^{-1}, 34.7 ± 0.4 μg g^{-1}, 5.1 ± 0.0 μg g^{-1}, and 970 ± 60 ng g^{-1}, respectively.

The data obtained for BHVO-2, NOD-A-1, and Allende are all in good agreement with the results reported in previous studies. The δ^{130}Te value obtained for NOD-P-1 in this study is consistent with some results obtained for this sample in previous studies, but higher than other published data. However, the large range of δ^{130}Te values reported in the literature for this sample, combined with intra-laboratory variability of δ^{130}Te seen in some previous studies, indicate that NOD-P-1 is somewhat heterogenous in relation to its Te isotope composition.

In addition to the previously categorised samples, this study reports the first precise analysis of the IAB-complex iron meteorite Canyon Diablo obtained using the double spike technique. This study also presents the first mass-dependent Te isotope composition and Te concentration data for the Alexo komatiite KAL-1, which were obtained using the double spike technique and isotope dilution.

The methods developed here hence allow accurate measurements of mass-dependent Te isotope composition in both high- and low-concentration terrestrial and extra-terrestrial samples using MC-ICP-MS. In addition, isotope mass balance and mixing equations were employed to show that possible mass-independent Te isotope effects in meteorites and terrestrial samples are unlikely to have a significant impact on measured δ^{130}Te values at the current level of analytical precision.

Author contributions

MR conceived the study and obtained funding. EMM developed and validated the method. EMM, KK, BJC, and GMP undertook the laboratory and mass spectrometry work. CJ and RM performed the nucleosynthetic Te modelling. EMM performed the NFSE Te modelling and calculated the impact of mass-independent Te isotope anomalies. EMM and MR developed the data reductions, performed the data interpretations, and wrote the manuscript.

Conflicts of interest

The authors declare no conflicts of interest.

Acknowledgements

This research was supported by UKRI STFC grant ST/W001179/1 to MR and a Hans Rausing PhD studentship to EMM. The authors would like to acknowledge Kirsty Crocket for providing the glacial till, Manuela Fehr for providing NIST SRM 3156 (lot no 892901) and ETH Te, and Jan Hellmann for providing NIST SRM 3156 (lot no 140830). The authors are grateful to the Natural History Museum London for providing the meteorite samples.

Notes and references

1 B. J. Wood, D. J. Smythe and T. Harrison, *Am. Mineral.*, 2019, **104**, 844–856.
2 M. A. Fehr, S. J. Hammond and I. J. Parkinson, *Geochim. Cosmochim. Acta*, 2018, **222**, 17–33.
3 J. L. Hellmann, T. Hopp, C. Burkhardt and T. Kleine, *Earth Planet. Sci. Lett.*, 2020, **549**, 116508.
4 J. L. Hellmann, T. Hopp, C. Burkhardt, H. Becker, M. Fischer-Gödde and T. Kleine, *Geochim. Cosmochim. Acta*, 2021, **309**, 313–328.
5 A. P. Fornadel, P. G. Spry, S. E. Jackson, R. D. Mathur, J. B. Chapman and I. Girard, *J. Anal. At. Spectrom.*, 2014, **29**, 623–637.
6 A. P. Fornadel, P. G. Spry, M. A. Haghnegahdar, E. A. Schauble, S. E. Jackson and S. J. Mills, *Geochim. Cosmochim. Acta*, 2017, **202**, 215–230.
7 A. P. Fornadel, P. G. Spry and S. E. Jackson, *Ore Geol. Rev.*, 2019, **113**, 103076.
8 Y. Fukami, J.-I. Kimura and K. Suzuki, *J. Anal. At. Spectrom.*, 2018, **33**, 1233–1242.
9 N. L. Wasserman and T. M. Johnson, *J. Anal. At. Spectrom.*, 2020, **35**, 307–319.
10 M. A. Fehr, M. Rehkämper and A. N. Halliday, *Int. J. Mass Spectrom.*, 2004, **232**, 83–94.
11 F. Wombacher and M. Rehkämper, *Geostand. Geoanal. Res.*, 2004, **28**, 173–178.
12 M. Rehkämper, F. Wombacher, T. J. Horner and Z. Xue, in *Handbook of Environmental Isotope Geochemistry*, ed. M. Baskaran, Springer, Berlin, Heidelberg, 2011, pp. 125–154.
13 J. F. Rudge, B. C. Reynolds and B. Bourdon, *Chem. Geol.*, 2009, **265**, 420–431.
14 E. Palk, R. Andreasen, M. Rehkämper, A. Stunt, K. Kreissig, B. Coles, M. Schönbächler and C. Smith, *Meteorit. Planet. Sci.*, 2018, **53**, 167–186.
15 G. M. Poole, M. Rehkämper, B. J. Coles, T. Goldberg and C. L. Smith, *Earth Planet. Sci. Lett.*, 2017, **473**, 215–226.
16 K. Murphy, M. Rehkämper, K. Kreissig, B. Coles and T. van de Flierdt, *J. Anal. At. Spectrom.*, 2016, **31**, 319–327.
17 X. Wang, C. Fitoussi, B. Bourdon and Q. Amet, *J. Anal. At. Spectrom.*, 2017, **32**, 1009–1019.
18 G. A. Brennecka, L. E. Borg, S. J. Romaniello, A. K. Souders, Q. R. Shollenberger, N. E. Marks and M. Wadhwa, *Geochim. Cosmochim. Acta*, 2017, **201**, 331–344.
19 M. Berglund and M. E. Wieser, *Pure Appl. Chem.*, 2011, **83**, 397–410.

20 G. M. Poole, R. Stumpf and M. Rehkämper, *J. Anal. At. Spectrom.*, 2022, **37**, 783–794.
21 M. A. Fehr, M. Rehkämper, A. N. Halliday, U. Wiechert, B. Hattendorf, D. Günther, S. Ono, J. L. Eigenbrode and D. Rumble, *Geochim. Cosmochim. Acta*, 2005, **69**, 5099–5112.
22 M. A. Fehr, M. Rehkämper, A. N. Halliday, M. Schönbächler, B. Hattendorf and D. Günther, *Geochim. Cosmochim. Acta*, 2006, **70**, 3436–3448.
23 M. A. Fehr, M. Rehkämper, A. N. Halliday, B. Hattendorf and D. Günther, *Meteorit. Planet. Sci.*, 2009, **44**, 971–984.
24 T. Fujii, F. Moynier and F. Albarède, *Chem. Geol.*, 2009, **267**, 139–156.
25 F. Moynier, T. Fujii and F. Albarède, *Meteorit. Planet. Sci.*, 2009, **44**, 1735–1742.
26 T. Fujii, F. Moynier and F. Albarede, *Earth Planet. Sci. Lett.*, 2006, **247**, 1–9.
27 S. Yang and Y. Liu, *Acta Geochim.*, 2016, **35**, 227–239.
28 M. Méheut, M. Ibañez-Mejia and F. L. H. Tissot, *Geochim. Cosmochim. Acta*, 2021, **292**, 217–234.
29 I. Angeli and K. P. Marinova, *At. Data Nucl. Data Tables*, 2013, **99**, 69–95.
30 D.-C. Lee and A. N. Halliday, *Int. J. Mass Spectrom. Ion Processes*, 1995, **146–147**, 35–46.
31 E. T. Mansur, S. Barnes, D. Savard and P. C. Webb, *Geostand. Geoanal. Res.*, 2020, **44**, 147–167.
32 Z. Wang and H. Becker, *Geostand. Geoanal. Res.*, 2014, **38**, 189–209.
33 Z. Zou, Z. Wang, H. Cheng, T. He, Y. Liu, K. Chen, Z. Hu and Y. Liu, *Geostand. Geoanal. Res.*, 2020, **44**, 501–521.
34 A. Forrest, R. Kingsley and J.-G. Schilling, *Geostand. Geoanal. Res.*, 2009, **33**, 261–269.
35 S. König, A. Luguet, J.-P. Lorand, F. Wombacher and M. Lissner, *Geochim. Cosmochim. Acta*, 2012, **86**, 354–366.
36 Z. Wang, H. Becker and F. Wombacher, *Geostand. Geoanal. Res.*, 2015, **39**, 185–208.
37 A. Yierpan, S. König, J. Labidi, T. Kurzawa, M. G. Babechuk and R. Schoenberg, *Geochem., Geophys., Geosyst.*, 2018, **19**, 516–533.
38 A. Yierpan, S. König, J. Labidi and R. Schoenberg, *Geochim. Cosmochim. Acta*, 2019, **249**, 199–224.
39 A. Yierpan, J. Redlinger and S. König, *Geochim. Cosmochim. Acta*, 2021, **313**, 155–172.
40 M. D. Axelsson, I. Rodushkin, J. Ingri and B. Öhlander, *Analyst*, 2002, **127**, 76–82.
41 T. Schirmer, A. Koschinsky and M. Bau, *Chem. Geol.*, 2014, **376**, 44–51.
42 G. G. Goles and E. Anders, *Geochim. Cosmochim. Acta*, 1962, **26**, 723–737.
43 L. Bonal, E. Quirico, M. Bourot-Denise and G. Montagnac, *Geochim. Cosmochim. Acta*, 2006, **70**, 1849–1863.